Scientific Paper

Evaluation of the Hydration of Portland Cement Containing Various Carbonates by Means of Thermal Analysis

Roman Gabrovšek[a], **Tomaž Vuk**[b], **Venčeslav Kaučič**[a]

[a] *National Institute of Chemistry, P. O. Box 660, SI-1001 Ljubljana, Slovenia*
[b] *Salonit Anhovo, Building Materials, Joint-Stock Co., SI-5210 Deskle, Slovenia*

Received 24-11-2005

Abstract

Portland cement containing a fixed amount of mineral admixtures (calcium carbonate or dolomite or magnesite) was hydrated at 60 °C for 7- and 28 days. Phase compositions were evaluated by thermogravimetric analysis and by powder X-ray diffraction. Measurements of surface area indicated the development of the hydrated microstructure. Detailed analysis of DTG decomposition profiles of portlandite and carbonate enabled the evaluation of certain admixture-related parameters concerning portlandite formation and also indicated the behavior of specific carbonates during the hydration process.

Keywords: Portland cement, admixture, carbonate, hydration, TG//DTG, decomposition profile.

Introduction

The production of Portland cement containing limestone, interground or blended with clinker, has increased particularly in the past decade due to technical and economical/environmental reasons. The technical reasons are satisfactory physical and mechanical properties of hydrated cement paste, and the economic/environmental reasons include energy saving during the decreased clinker production and consequently the reduction of environmental pollution by carbon dioxide. The European standard EN 197-1 and the adopted Slovenian standard SIST EN 197-1 allow up to 35 wt % of limestone in cement.[1]

During the hydration of Portland cement clinker minerals react with water yielding a complex microstructure consisting mainly of amorphous calcium silicate hydrate gel (approx. $1.7CaO{\cdot}SiO_2{\cdot}1.5H_2O$; C-S-H in cement chemistry notation), ettringite ($3CaO{\cdot}Al_2O_3{\cdot}3CaSO_4{\cdot}32H_2O$), portlandite ($Ca(OH)_2$), carbonated phases and calcite ($CaCO_3$). When limestone is present in Portland cement, the rate and degree of hydration change, as does the composition of the hydrated cement paste. The literature findings on the effect of limestone on the composition of hydrated cement paste are not always in close agreement but the general conclusion is that limestone participates to a certain extent in chemical reactions during hydration, not being only an inert filler.[2]

The purpose of our research was the investigation of the effects of various carbonates on 7- and 28-day hydration of Portland cement. The composition of hydrated cement paste was evaluated by thermogravimetric/derivative thermogravimetric analysis (TG/DTG) which has had a long tradition in studies on hydrated cements.[3-8] Scientific literature contains an ample amount of papers dealing with the applications of thermal analysis (TG/DTG-DTA or DSC) to broad aspects of the cement hydration process and its chemistry although most studies are necessarily specifically oriented to coincide with the purpose of a particular research topic.[9-17] Hydrated samples were also analyzed by powder X-ray diffraction and the evolution of microstructure was assessed by the measurement of surface area. The emphasis was, however, placed on the study of DTG (mass loss rate) profiles due to their great sensitivity for the determination of specifics of hydrated cement phases when compared with X-ray diffraction method.

Experimental

Portland cement used was CEM I 52.2 R, Salonit Anhovo, Building Materials, Joint-Stock Co., Anhovo, Slovenia. Table 1 shows chemical and mineralogical analyses of the cement used.

The addition of carbonates was 15% in all cases to facilitate comparison (constant amount of hydrating Portland cement).

Table 1. Chemical and mineralogical analysis of CEM I 52.2 R.

Chemical analysis		Mineralogical analysis*	
CaO:	63.3%	C_3S:	54.9%
SiO_2:	20.6%	C_2S:	17.7%
Al_2O_3:	4.71%	C_3A:	6.6%
Fe_2O_3:	3.50%	C_4AF:	10.7%
SO_3:	3.37%		
MgO:	1.12%		
K_2O:	0.87%		
Na_2O:	0.21%		
LOI:	1.90%		
Insoluble:	0.37%		

*Standard cement chemistry notations: C: CaO; S: SiO_2; A: Al_2O_3; F: Fe_2O_3.

Three kinds of $CaCO_3$ were used:

Laboratory reagent, $CaCO_3$, 99.1%, Kemika, Zagreb, Croatia. Specific surface area of 0.7 m^2/g. Designated as *$CaCO_3$ p.a.* further in the text.

Natural, ground calcite, $CaCO_3$, 99.6%, Magnesia 448, Magnesia GmbH, Lüneburg, Germany. Specific surface area of 2.1 m^2/g (micropore area: 0.3 m^2/g). Designated as *calcite* further in the text.

Natural, ground limestone, $CaCO_3$, 98.7%, Salonit Anhovo, Building Materials, Joint-Stock Co., Anhovo, Slovenia. Specific surface area of 2.2 m^2/g (micropore area: 0.3 m^2/g). Designated as *limestone* further in the text.

Additionally, the following two carbonates were also used in the investigation:

Natural, ground dolomite, $CaMg(CO_3)_2$, 99.5%, Magnesia 4179, Magnesia GmbH, Lüneburg, Germany. Specific surface area of 1.7 m^2/g (micropore area: 0.2 m^2/g). Designated as *dolomite* further in the text.

Natural, ground magnesite, $MgCO_3$, 98.1%, Magnesia 318, Magnesia GmbH, Lüneburg, Germany. Specific surface area of 4.6 m^2/g (micropore area: 1.0 m^2/g). Designated as *magnesite* further in the text.

Figures 1 and 2 show carbonate decomposition profiles and corresponding characteristic temperatures of calcium carbonates, magnesite and dolomite.

Portland cement and added carbonate were homogenized and distilled water (w/s ratio of 5) was added. Suspensions were hydrated at 60 °C for 7 and 28 days (further designated as *7d* and *28d*, respectively, in the text). The hydration in suspension at 60 °C was chosen with an intention of enhancing the first stage (known as the solution phase) of cement hydration where ettringite and later calcium silicate hydrates form.

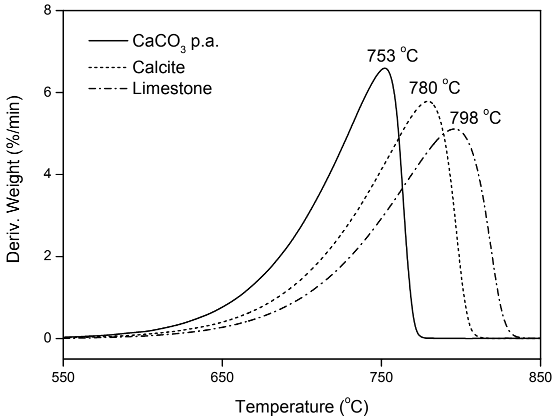

Figure 1. DTG decomposition profiles of $CaCO_3$ p.a., calcite and limestone.

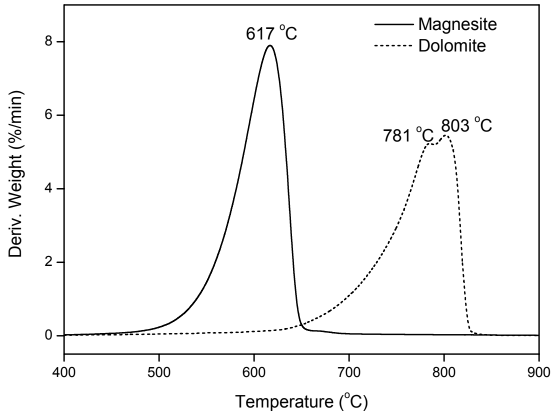

Figure 2. DTG decomposition profiles of dolomite and magnesite.

Hydrated samples were washed with ethanol and diethyl ether and dried overnight in a forced-air oven at 40 °C.

Portland cement hydrated under the same conditions was used as a reference.

Thermal analyses were run on a SDT 2960 Simultaneous DSC-TGA instrument (TA Instruments – Waters LLC, USA) at 10 °/min from 25 to 800 °C in 100 mL/min N_2 flow. All results in the paper are given in terms of the ignited mass, i. e. the experimental results of mass losses were recalculated with regard to the remaining mass of ignited cement at 800 °C for each sample investigated. This correction facilitates comparisons among samples having different mass losses.

Powder X-ray diffraction was performed on Siemens D5000 instrument (Siemens, Germany) with Cu Kα radiation from 5 to 65 °2ϑ with a step of 0.03° and with 5 s/step.

Surface areas were determined by an automatic gas adsorption analyzer (TriStar 3000, Micromeritics Instrument Corp., USA). A standard 5-point BET method, based on N_2 adsorption at 77 K, was used.

Results and Discussion

Figures 3 and 4 show characteristic shapes of TG/DTG curves of anhydrous cement and its hydrated form, respectively.

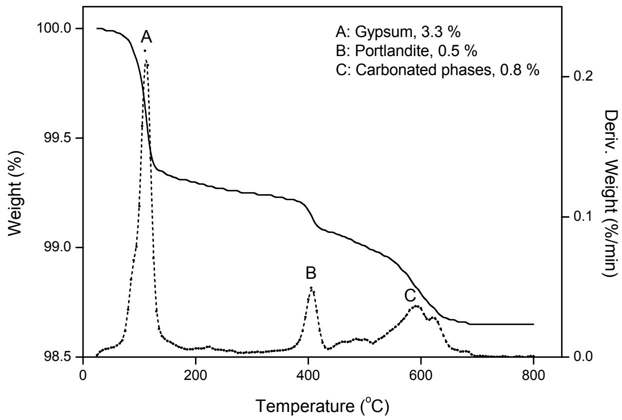

Figure 3. TG/DTG curve of anhydrous cement.

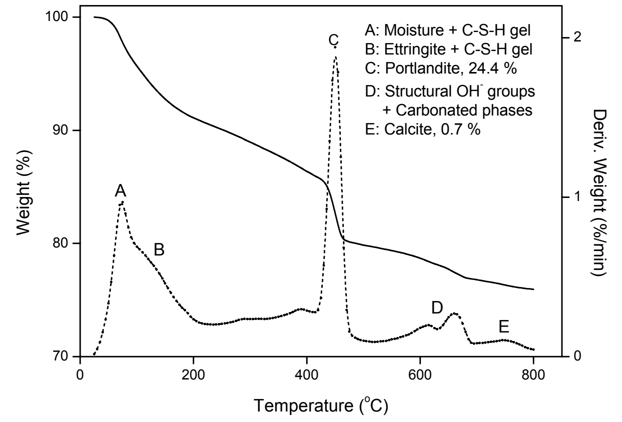

Figure 4. TG/DTG curve of cement hydrated for 28 days at 60 °C.

Anhydrous cement contains gypsum, $CaSO_4 \cdot 2H_2O$ (added as a set regulator during cement production); the presence of small quantities of portlandite, $Ca(OH)_2$, and carbonated phases (amorphous and finely divided calcite, $CaCO_3$) is a consequence of the reaction of cement with atmospheric air during storage.

Hydrated cement shows a significant mass loss up to 200 °C attributed to surface water desorption as well as water loss from C-S-H gel layers and from the dehydration of ettringite. Further mass loss up to approx. 400 °C indicates continuous thermal decomposition of a complex mixture of hydrated silicate- and aluminate-type compounds. Next, thermal decomposition of portlandite, $Ca(OH)_2$, takes place followed by the decomposition of carbonated phases and calcite, $CaCO_3$. The exact amount of carbonated phases can not be reliably calculated from the mass loss data because structural OH^- groups from C-S-H gel also contribute to measured mass loss within this temperature interval.

Cement without additions

Total mass losses of 7d and 28d cements were 19.3 and 21.9%, respectively. Although TG curves are similar in shape, significant differences can be observed in DTG profiles of portlandite and carbonated phases decompositions.

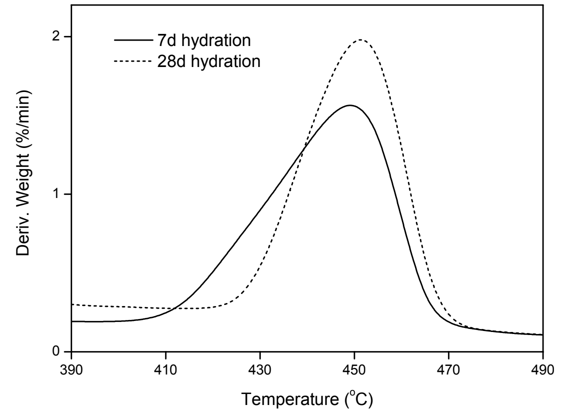

Figure 5. DTG profiles of portlandite dehydration.

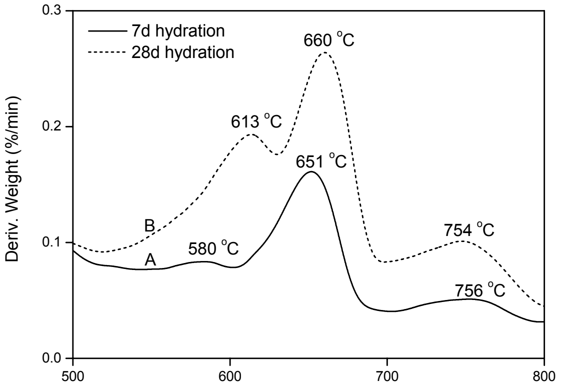

Figure 6. DTG profiles of carbonated phases decomposition.

The dehydration profile of portlandite (Fig. 5) from 7d cement is broader than the corresponding profile from the 28d sample (Full Width at Half-Maximum, FWHM, of 30 °C and 24 °C, respectively) and exhibits lower onset temperature (414 °C and 428 °C, respectively). Portlandite contents (23.0±0.3%)

and peak decomposition temperatures (451±1 °C) are, however, equal for both samples. It is, therefore, evident that portlandite converts to a more crystallized form (or larger crystals via Ostwald ripening) during increased time of hydration.

Carbonated phases decompose (Fig. 6) in a broad temperature interval from 500 to 800 °C. The sample of 7d cement shows a small mass loss due to structural OH^- groups from C-S-H gel (DTG_{max} at 580 °C) and mass losses due to amorphous carbonated phases (DTG_{max} at 651 °C) and well-crystallized calcite (DTG_{max} at 754 °C). The sample of 28d cement shows increased mass loss resulting from an increased content of C-S-H gel structural OH^- groups; the peak has been shifted to a higher temperature (DTG_{max} at 613 °C) due to improved ordering of the C-S-H gel structure after the longer hydration time. The peak due to the carbonated phases has narrowed and shifted to a higher temperature (DTG_{max} at 660 °C) and the peak area of well-crystallized calcite has doubled.

X-ray diffraction and surface areas:

Portlandite, calcite, ettringite, traces of calcium monosulfoaluminate hydrate ($3CaO{\cdot}Al_2O_3{\cdot}CaSO_4{\cdot}12H_2O$) and unreacted alite ($3CaO{\cdot}SiO_2$) were identified in 7d and 28d cements. Contents of calcite and ettringite increased with longer hydration time. Portlandite content, however, decreased due to its conversion to carbonated phases and calcite.

Surface areas for 7d and 28d cements increased from 47.5 to 66.0 m^2/g due to the development of C-S-H phases with hydration time.

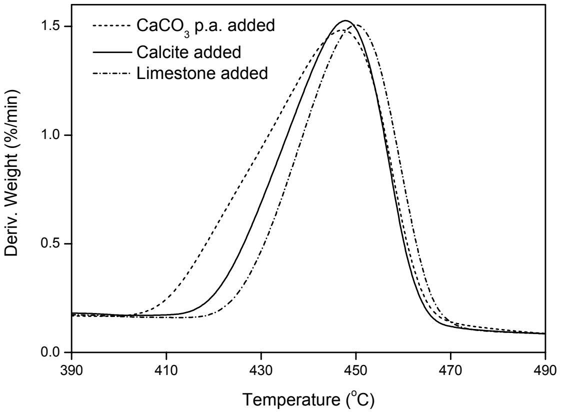

Figure 7. DTG profiles of portlandite of 7-day hydrated cement with carbonate additions.

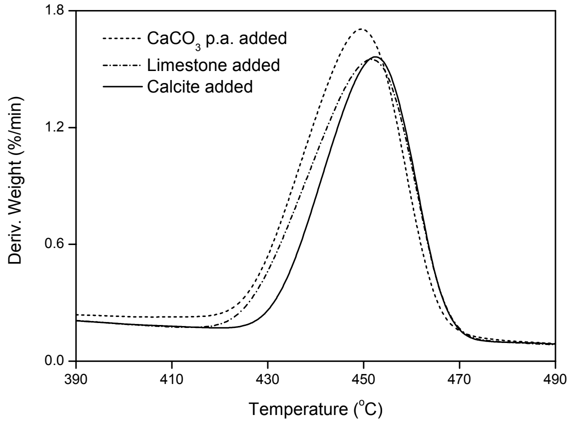

Figure 8. DTG profiles of portlandite of 28-day hydrated cement with carbonate additions.

Cement with added carbonates

Total mass losses for 7d and 28d cements with the additions of various carbonates were 23.4±1.0 and 25.5±0.9%, respectively.

Portlandite decomposition profiles for hydrated carbonate-containing cements are shown in Figures 7 and 8.

The DTG profile of portlandite from the 7d cement with the addition of $CaCO_3$ p.a. (Fig. 7) differs from the other two DTG profiles. It has a broad decomposition interval (FWHM of 31 °C) and lower dehydration onset (411 °C). The profile is almost identical to the DTG profile of portlandite from pure hydrated cement. The remaining two DTG profiles of portlandite (hydrated cement containing calcite and limestone) are similar to each other (FWHM of 23 °C and dehydration onset of 423±2 °C). It seems that nonporous, low-surface area $CaCO_3$ p.a. acts rather ineffectively in modifying the portlandite formed.

DTG profiles of portlandite from 28d cements with carbonate added (Fig. 8) show less variability than corresponding 7d samples. Portlandite from hydrated cement with calcite added appears to be more crystalline than the other two: it has narrower decomposition interval (FWHM of 21 °C) and higher dehydration onset (431 °C).

Portlandite content is somewhat lower in 28d cements, 18-21%, when compared with 7d cements, 19-23%. Decomposition peak maxima (DTG_{max} at 450±2 °C) are similar for all samples.

DTG profiles of carbonated phases and carbonates, shown in Figures 9 and 10, are difficult to evaluate due to a series of overlapped decompositions of substances with unknown stoichiometry (structural OH^- groups from C-S-H gel and anhydrous and hydrated carbonate phases). Only general conclusions are thus possible from the shape of DTG profiles.

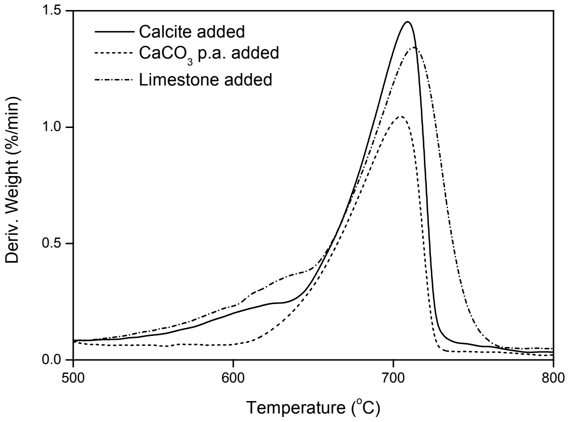

Figure 9. DTG profiles of 7-day hydrated cement with carbonates added.

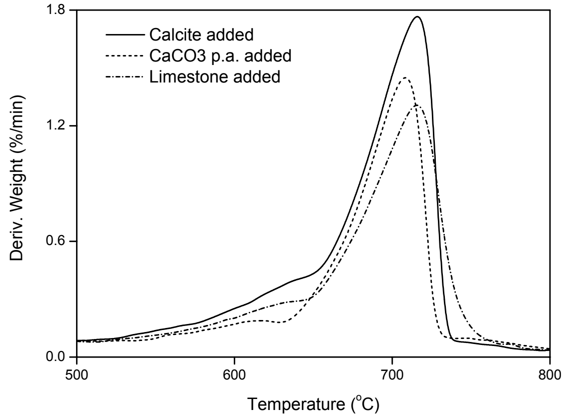

Figure 10. DTG profiles of 28-day hydrated cement with carbonates added.

We can conclude (Fig. 9) that 7d cement with added CaCO$_3$ p.a. does not contain any appreciable quantity of carbonated phases (preceding the main calcite peak) in sharp contrast to the other two samples. Temperatures of peak decomposition maxima are significantly lower (50-70 °C) for each carbonate if compared with corresponding decomposition temperatures of individual carbonates (Fig. 1).

DTG profiles of the carbonated part of 28d cements (Fig. 10) follow a similar trend as in Fig.9. The difference can, however, be seen in the presence of carbonated phases also in the sample containing CaCO$_3$ p.a.

X-ray diffraction and surface areas:

The same phases as in hydrated cements without additions were identified, although with different contents and time dependencies. There was, however, no unreacted alite which was a consequence of a known acceleratory influence of calcium carbonate(s) on the alite hydration kinetics.

Surface areas increased from 41.0±0.5 to 46.0±0.5 m^2/g for 7d and 28d cements, respectively.

Cement with added dolomite and magnesite

Total mass losses (at 800 °C) for 7d hydrated cements with dolomite and magnesite additions were 25.3 and 24.4%, and for 28 d hydrated cements the corresponding values were 27.0 and 26.2%.

Portlandite decomposition patterns for samples with dolomite and magnesite added are shown in Figures 11 and 12, respectively.

Both 7d and 28d cements with dolomite added (Fig. 11) show the presence of brucite, Mg(OH)$_2$ that formed due to an alkali carbonate reaction during the hydration. Brucite contents increases with longer hydration time (from 0.4 to 0.7%).

Hydrated cements with magnesite added (Fig. 12) show significant amounts of brucite formed (2% for 7d and 3.7% for 28d cements) and the corresponding decrease in portlandite content (16% for 7d and 11% for 28d cements).

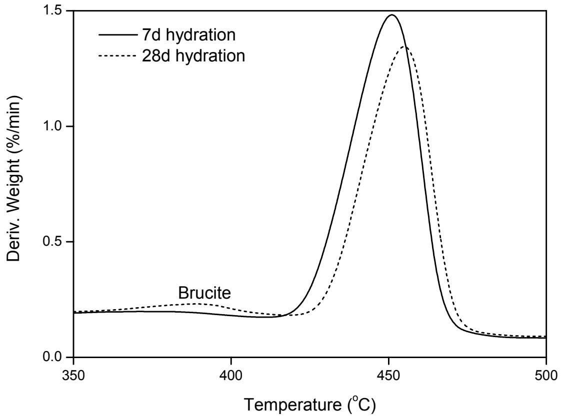

Figure 11. DTG profile of portlandite of hydrated cement with dolomite added.

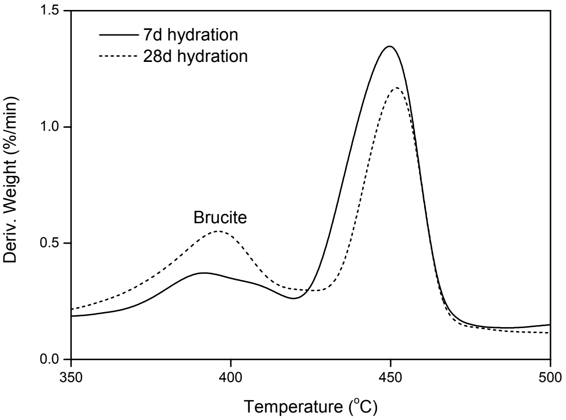

Figure 12. DTG profile of portlandite of hydrated cement with magnesite added.

Portlandite decomposition profiles, in terms of peak maxima, temperature intervals and FWHM, are similar for all samples and appear to be independent of the addition of either dolomite or magnesite.

DTG profiles of the carbonate region of samples are shown in Figures 13 and 14.

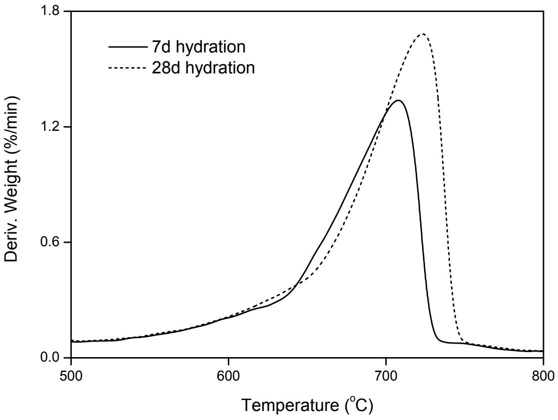

Figure 13. DTG profiles of carbonate region of hydrated cement with dolomite added.

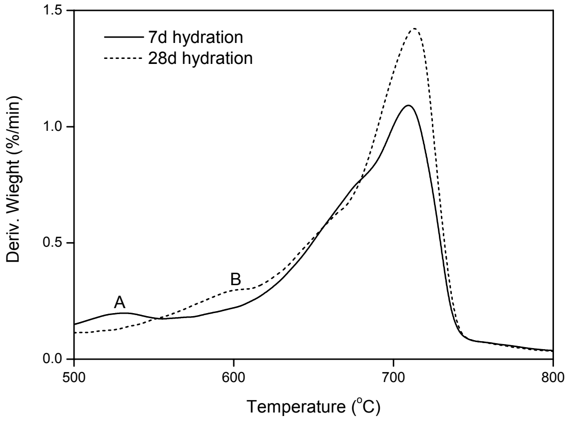

Figure 14. DTG profiles of carbonate region of hydrated cement with magnesite added.

Decomposition profiles of carbonate from hydrated cements with dolomite added (Fig. 13) show no distinct features. Continuous mass loss extends from 500 to 800 °C. The temperatures of single peak maxima are, however, significantly lower in comparison with the original magnesite doublet (DTG_{max} at 708 and 728 vs. 781+803 °C, Fig. 2).

Contrary to the above, carbonate decomposition profiles of magnesite-containing cements show several, time-dependent features: 7d cement shows mass loss at 530 °C (A, Fig. 14) that shifts to 600 °C (B, Fig. 14) after 28-day hydration; both main carbonate peaks of $CaCO_3$ decomposition show a shoulder on their lower-temperature side corresponding to the remaining magnesite that has not converted to brucite. The observed shoulders also shift to higher temperature with longer hydration time.

X-ray diffraction and surface areas:

X-ray diffraction scans showed the presence of all phases that were also detected by thermogravimetric analysis.

Surface areas of dolomite-containing cement paste did not change much, from 42.4 (7d) to 42.8 m^2/g (28d) but the measurement for 28d cement indicated that 2.3 m^2/g of surface area originated from micropores that formed in the hydrated cement.

Surface areas of magnesite-containing cement paste increased from 40.0 to 47.0 m^2/g with longer hydration time.

Conclusions

The hydration of Portland cement containing several carbonates was evaluated by the use of DTG profiles. This approach offers the advantage to study, besides the usual mass losses and characteristic temperatures obtained from TG curves, also important peak parameters such as onset temperature, peak width and asymmetry and peak shoulders. These parameters supply additional information on portlandite and carbonate behavior in hydrating cement environments that can not be evaluated by analyzing TG curves.

The effect of several calcium carbonates that differ in $CaCO_3$ content and in surface area on the hydration of cement is that nonporous $CaCO_3$ p.a., having low surface area, significantly impedes the crystallization of portlandite, particularly at shorter hydration times. Lower reactivity of $CaCO_3$ p.a. is also evident from the absence of any carbonated low-crystalline phases preceding the main calcite decomposition peak. Variable crystallinity of portlandite formed can exhibit different carbonation rates and thus consequently affects the final porosity of cement paste. These features could not be evaluated by the use of X-ray diffraction due to its known shortcomings (particularly with regard to amorphous content of samples and portlandite preferred orientation problems) when used in the quantitative investigation of hydrated cement phases.

The effects of dolomite and magnesite addition on cement hydration are unambiguous for dolomite addition but, nevertheless, more complicated in the case of magnesite addition. In both cases, as a consequence of an alkali-carbonate reaction between Mg^{2+} and portlandite, varying amounts of brucite form which is known to have a deleterious expansive effect on already hardened cement paste if present in larger quantities. The carbonate decomposition profile of magnesite-containing hydrated cement shows a rather complex, time-dependent profile that is a consequence of magnesite alkali-carbonate disproportionate reaction into brucite, calcite and remaining magnesite.

Acknowledgment

The authors thank the Slovenian Research Agency for funding this research (Grant P1-0021).

The authors also thank Magnesia GmbH, D-21311 Lüneburg, Germany, for donating calcite, dolomite and magnesite samples for this study.

References

1. European Committee for Standardization; Cement: Composition, Specifications and Conformity Criteria, Part 1: Common Cements, EN 197-1 (**2000**)
2. P. Hawkins, P. D. Tennis, R. Detwiler, The Use of Limestone in Portland Cement: A State-of-the-Art Review, EB 227, Portland Cement Association, Skokie**,** **2003**, 44 pp.
3. V. S. Ramachandran, Applications of Differential Thermal Analysis in Cement Chemistry, Chemical Publishing Company, Inc., New York, **1969**, 307 pp.
4. T. L. Webb, J. E. Krüger, in: R. C. Mackenzie (Ed.): Differential Thermal Analysis, Vol. 2, Academic Press, London, **1972**, pp. 181–205.
5. R. Barta, in: R. C. Mackenzie (Ed.): Differential Thermal Analysis, Vol. 2, Academic Press, London, **1972**, pp. 207–228.
6. V. S. Ramachandran, in: V. S. Ramachandran, J. J. Beaudoin (Eds.): Handbook of Analytical Techniques in Concrete Science and Technology, William Andrew Publishing, Norwich, **2001**, pp. 127–173.
7. S. K. Handoo, in: S. N. Ghosh (Ed.): Advances in Cement Technology: Chemistry, Manufacture and Testing, 2nd Edition, Tech Books International, New Delhi, **2002**, pp. 631–659.
8. V. S. Ramachandran, R. M. Paroli, J. J. Beaudoin, A. H. Delgado (Eds.): Handbook of Thermal Analysis of Construction Materials, Noyes Publications, Norwich, **2003**, 680 pp.
9. P. Longuet, Rev. Mater. Constr. Trav. Publ. **1960**, No. 537, 538–540.
10. V. S. Ramachandran, Thermochim. Acta **1972**, *3*, 343–366.
11. B. El-Jazairi, J. M. Illston, Cem. Concr. Res. **1980**, *10*, 361–366.
12. V. S. Ramachandran, Thermochim. Acta **1988**, *127*, 385–394.
13. S. Tsivilis, G. Kakali, E. Chaniotakis, A. Souvaridou, J. Therm. Anal. **1998**, *52*, 863–870.
14. M. A. Helal, Cem. Concr. Res. **2002**, *32*, 447–450.
15. J. Dweck, P. F. Ferreira da Silva, P. M. Büchler, F. K. Cartledge, J. Therm. Anal. Calorim. **2002**, *69*, 179–186.
16. V. Rahhal, R. Talero, Cem. Concr. Res. **2005**, *35*, 1285–1291.
17. N. Voglis, G. Kakali, E. Chaniotakis, S. Tsivilis, Cem. Concr. Comp. **2005**, *27*, 191–196.

Povzetek

Portland cement s konstantno vsebnostjo mineralnih dodatkov (kalcit, dolomit in magnezit) smo hidratizirali 7- in 28 dni v suspenziji pri 60 °C. Fazne sestave hidratiziranih produktov smo ovrednotili s termogravimetrično analizo in s praškovno rentgensko difrakcijo, razvoj hidratizirane mikrostrukture pa smo ugotavljali z merjenjem specifične površine. Z detajlno analizo DTG profilov termičnega razpada portlandita in karbonata smo ugotovili določene vplive mineralnih primesi na nastanek portlandita. V procesu hidratacije smo ovrednotili tudi specifično obnašanje posameznih prisotnih karbonatov.